Evaluation of disulfide reduction during receptor-mediated endocytosis by using FRET imaging

Jun Yang*, Hongtao Chen*†, Iontcho R. Vlahov‡, Ji-Xin Cheng*†, and Philip S. Low*§

*Department of Chemistry and †Weldon School of Biomedical Engineering, Purdue University, West Lafayette, IN 47907; and ‡Endocyte, Inc., West Lafayette, IN 47906

Edited by Roger Y. Tsien, University of California at San Diego, La Jolla, CA, and approved June 2, 2006 (received for review February 22, 2006)

Despite functional evidence for disulfide bond-reducing activity in endosomal compartments, the mechanistic details pertaining to such process (e.g., kinetics and sites of disulfide reduction) remain largely controversial. To address these questions directly, we have synthesized a previously uncharacterized fluorescent folate conjugate, folate-(BODIPY FL)-SS-rhodamine (folate-FRET), that changes fluorescence from red to green upon disulfide bond reduction. Using this construct, we have observed that disulfide reduction: (*i*) occurs with a half-time of 6 h after folate-FRET endocytosis, (*ii*) begins in endosomes and does not depend significantly on redox machinery located on the cell surface or within the lysosome or the Golgi apparatus, (*iii*) occurs independently of endocytic vesicle trafficking along microtubules, and (*iv*) yields products that are subsequently sorted into distinct endosomes and trafficked in different directions. Finally, colocalization of folate and transferrin receptors suggest that conclusions derived from this study may apply to other endocytic pathways.

disulfide bond reduction | endosome | folate receptor | drug targeting

It is generally accepted that a large redox potential difference exists across the plasma membrane of most mammalian cells. Thus, an intracellular excess of reduced glutathione (GSH), thioredoxin, peroxiredoxins, and nicotinamide adenine dinucleotides (NADH and NADPH) over their oxidized counterparts assures that the cytosol remains highly reducing despite an oxidizing extracellular milieu (1–4). Separate from the cytosolic space, however, the lumen of some intracellular organelles may be somewhat oxidizing. The endoplasmic reticulum, for example, has a relatively low GSH/glutathione disulfide or oxidized glutathione ratio and, thereby, allows formation of disulfide bonds in secreted proteins or proteins exposed on exoplasmic cell surfaces (5).

Evidence also exists that some intracellular organelles may possess a reductive capacity that enables the noncytosolic cleavage of disulfide bonds. Activation of diphtheria toxin (DT) after endocytosis, for example, requires the acid-triggered exposure of an interchain disulfide bond that must be reduced before endosomal escape and cell killing can occur (6–8). Importantly, blockade of cell surface sulfhydryls (SHs) has been shown to inhibit activation of DT, suggesting that reduction of the critical disulfide bond may be mediated by SHs that originally were present at the cell surface, but through endocytosis, became oriented at the inner face of the nascent endosome. Intracellular reduction of disulfide bonds in Cholera toxin and *Pseudomonas* exotoxin also appear to be required for expression of cytotoxic activity (9). In an effort to more precisely determine the nature and location of the endosomal/organellar redox activity, Feener *et al.* (10) constructed a membrane absorptive polymer, [^{125}I]-tyramine-SS-poly-D-lysine and measured the appearance of its reduced counterpart in various subcellular fractions after cell fragmentation and Percoll gradient separation. When applied to CHO cells, cleavage of the disulfide construct began without a lag period and continued for >6 h, yet it was partially inhibited by membrane impermeable SH blockers, such as 5,5′-dithiobis-(2-nitrobenzoic acid) and *p*-chloromercuribenzenesulfonic acid (pCMBS). These data suggest that disulfide bond reduction can begin on the exofacial surface of the cell but must continue for some time after endocytosis. Because reduction of this conjugate also was found to be vulnerable to both an inhibitor (bacitracin) and an antibody against protein disulfide isomerase (PDI), involvement of plasma membrane-bound PDI was strongly implicated (11). However, the fact that the inhibition only was partial even at saturating concentrations of impermeant inhibitors suggests that a second phase of reduction must take place somewhere inside the cell (10).

Although these pioneering studies provided substantial evidence for reductive activity within the endocytic pathway, the techniques used did not permit a highly resolved picture of where and when intraendosomal disulfide bond reduction occurs. Thus, endosome fragmentation and mixing during cell homogenization and gradient centrifugation can lead to cross-contamination of subcellular fractions with similar biophysical properties (e.g., late endosome and recycling endosome). Moreover, the simple process of cell homogenization and organelle extraction/isolation could conceivably alter redox activities, and rupture of membrane boundaries separating compartments of different redox potentials could leak reducing components into nonreducing compartments or vice versa. Therefore, a real-time, noninvasive method for detection of intraendosomal disulfide bond reduction under normal physiological conditions has the potential to enhance our understanding of disulfide reduction during normal intracellular trafficking.

In this paper, we present a previously uncharacterized strategy for real-time visualization of disulfide bond cleavage in live cells during receptor-mediated endocytosis. For ease of analysis, we have examined the endocytic pathway followed by the folate receptor (FR), a glycosylphosphatidylinositol-anchored protein that is responsible for folate uptake in some mammalian cells (12). After FR binding, folate is thought to be internalized into vesicular endosomes called glycosylphosphatidylinositol-anchored protein-enriched endosomal compartments (13, 14) and, then, after trafficking to a recycling endosomal compartment (REC) that also can process receptors that internalize at clathrin-coated pits, FR is believed to be sorted and ultimately escorted back to the cell surface (15, 16).

A variety of folate-linked fluorescent dyes have long been used to study FR-mediated endocytosis, largely due to the high affinities (K_d = 1–10 nM) and high specificities of folate conjugates for FR (17, 18). In this study, we describe the synthesis and use of a disulfide-linked folate conjugate that selectively binds FR ($K_d \approx 10$ nM) and changes fluorescence from red to green upon disulfide

Conflict of interest statement: No conflicts declared.

This paper was submitted directly (Track II) to the PNAS office.

Abbreviations: BODIPY, 4,4-difluoro-5,7-dimethyl-4-bora-3*a*,4*a*-diaza-*s*-indacene-3-propionic acid; FR, folate receptor; PDI, protein disulfide isomerase; REC, recycling endocytic compartment; SH, sulfhydryl; Tf, transferrin; TfR, transferrin receptor.

§To whom correspondence should be addressed. E-mail: plow@purdue.edu.

www.pnas.org/cgi/doi/10.1073/pnas.0601455103

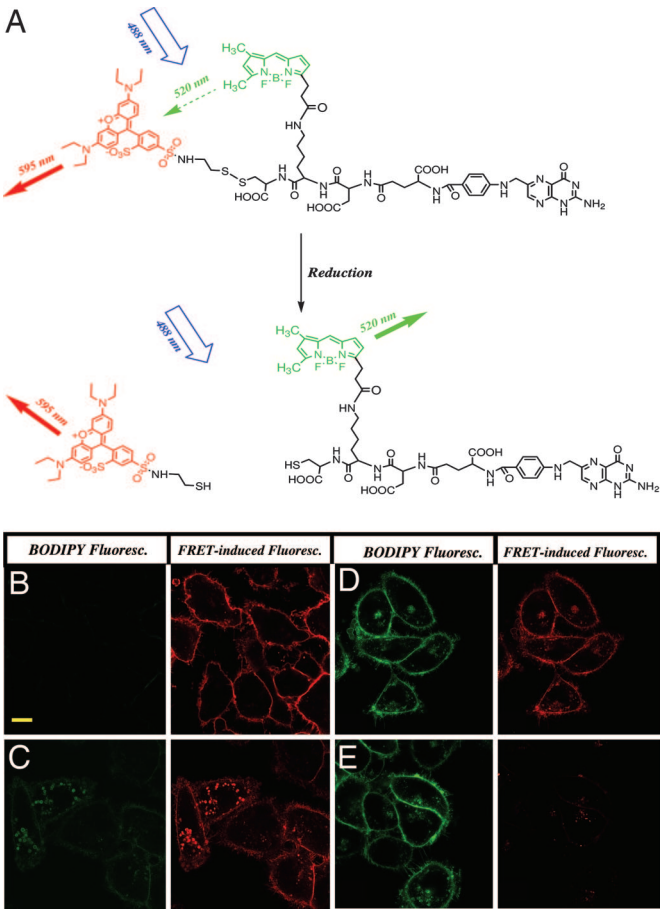

Fig. 1. The folate-FRET reporter changes fluorescence from red to green upon disulfide reduction. (*A*) Disruption of intramolecular energy transfer in the folate-FRET reporter by disulfide reduction. In the nonreduced folate-FRET reporter (*Upper*), excitation of BODIPY FL (BODIPY) leads to rhodamine (red) emission due to FRET from BODIPY to rhodamine. Upon disulfide reduction, rhodamine is released from the folate-BODIPY backbone, leading to loss of FRET (red) fluorescence and concurrent recovery of BODIPY (green) fluorescence. (*B–E*) FRET images of KB cells after incubation for different lengths of time with folate-FRET reporter. Cells were incubated for 0.5 h with the folate-FRET (100 nM) and washed to remove unbound conjugate. Cells then were imaged immediately (*B*) or after 2 (*C*), 6 (*D*), or 12 (*E*) h of further incubation in culture medium by excitation at 488 nm with confocal microscopy. In these images, the intact folate-FRET reporter molecule appears red, and the reduced folate-BODIPY fragment appears green. (Scale bar: 10 μm.)

bond reduction. Using this construct, we provide real-time visualization of disulfide reduction during folate receptor-mediated endocytosis, and we exploit this capability to characterize the intracellular locations where disulfide bond reduction can take place.

Results

Characterization of the Disulfide-Linked Folate-FRET Reporter. As depicted in Fig. 1*A*, the folate-FRET reporter used in this study is comprised of (*i*) folic acid, the high-affinity ligand for FR; (*ii*) a hydrophilic peptide spacer that improves the conjugate's water solubility and provides a backbone for fluorophore attachment; 3) the FRET donor, 4,4-difluoro-5,7-dimethyl-4-bora-3*a*,4*a*-diaza-*s*-indacene-3-propionic acid (BODIPY) FL (488/520 nm), which is linked to folate via an amide bond; and (*iv*) the FRET acceptor, tetraethyl rhodamine (545/595 nm) that is linked to folate via the reducible disulfide bond. The probe is designed such that the two fluorophores (BODIPY and rhodamine) are attached to folate in close proximity, resulting in efficient intramolecular energy transfer. Upon reduction, disulfide-linked rhodamine is released from the folate conjugate, whereas BODIPY remains attached through the amide bond. This separation of fluorophores leads to loss of FRET.

To test the validity of this design, the folate FRET reporter was treated with reducing agent, and reduction was monitored by both HPLC and fluorescence spectrophotometry. As seen in Fig. 7*A*, which is published as supporting information on the PNAS web site, the intact FRET reporter appears as a single peak on reverse-phase HPLC and exhibits absorbance maxima at both 504 nm (BODIPY) and 575 nm (rhodamine), indicating the presence of both fluorophores on the same molecule. When excited at 488 nm, the intact folate-FRET reporter was found to emit primarily at 595 nm (red fluorescence) as a consequence of efficient intramolecular energy transfer from BODIPY to rhodamine (Fig. 7*B*). In contrast, after treatment with the inorganic reductant, tri(2-carboxyethyl)phosphine hydrochloride (TCEP), the folate-FRET reporter was found to be cleaved at its disulfide bridge, generating two distinct peaks on HPLC that absorbed independently at 504 (folate-BODIPY) and 575 nm (free rhodamine) (Fig. 7*A*). Excitation of this reduced conjugate at 488 nM yielded only the green emission of the BODIPY fluorescence (Fig. 7*B*). Thus, reduction of the folate-FRET reporter results in a change from red to green emission upon excitation at 488 nm.

Kinetics of Disulfide Cleavage of Folate-FRET Reporter in KB Cells. To obtain an initial indication of the rate and location of disulfide bond reduction during endosomal trafficking, FR-expressing KB cells were incubated with the folate-FRET conjugate for various times, and the distribution of red (595 nm channel) and green (520 nm channel) fluorescence was analyzed by confocal microscopy. At 30 min of incubation (Fig. 1*B*), strong red fluorescence was observed on the plasma membrane with some red fluorescence detectable in cell periphery. Green fluorescence, in contrast, was indistinguishable from background levels measured in control experiments, indicating that even those few folate-FRET reporters that already had internalized still remained intact. By 2 h of incubation (Fig. 1*C*), however, much of the FRET conjugate had moved from the plasma membrane to a perinuclear region, presumably the REC that has been shown by others to constitute a site for processing glycosylphosphatidylinositol-anchored proteins (14). Concurrent with this trafficking to the perinuclear region, green fluorescence began to appear in this area, even though the red fluorescence remained dominant throughout the cell. This observation suggests that disulfide reduction may begin either before or during accumulation at the REC.

As the incubation period proceeded, red fluorescence intensity continued to decline, whereas green fluorescence steadily increased throughout the cell. By 6 h of incubation, green fluorescence was not only strongly visible in endosomes, but also over the entire cell surface (Fig. 1*D*). Unfortunately, careful analysis of multiple micrographs obtained at various intermediate time points could not reveal whether the green fluorescence on the cell surface arose as a consequence of: (*i*) folate-FRET reporter that was reduced in an endosomal compartment and subsequently recycled to the cell surface, or (*ii*) folate-FRET reporter that never internalized but still was reduced by some type of exofacial redox activity. Finally, by 12 h of incubation, virtually all red fluorescence had converted to green (Fig. 1*E*), suggesting that few disulfide bonds persisted in the folate-linked reporter.

To more quantitatively assess the kinetics of disulfide reduction, cell-associated fluorescence (excited at 488 nm) was analyzed by flow cytometry (FACS) as a function of incubation time. For this purpose, the ratio of red to the sum of red and green fluorescence [i.e., red/(red + green)] was quantitated as a measure of the ratio of reduced to intact folate-FRET reporters in the cell. As shown in Fig. 2, disulfide reduction proceeded exponentially throughout the 12-h observation period. Analysis of the kinetics yielded a half-time

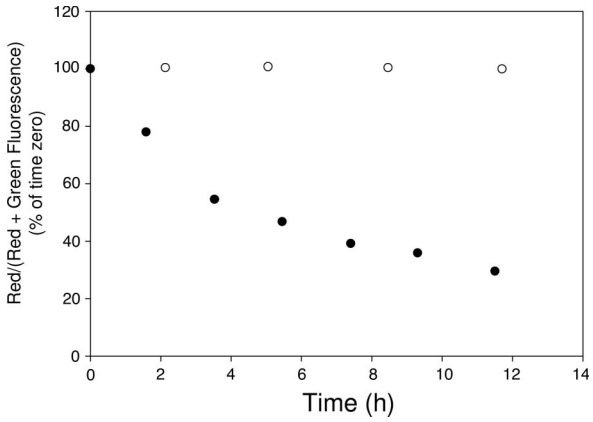

Fig. 2. Time course of disulfide cleavage of the folate-FRET reporter in KB cells. Changes in the ratio of red (intact FRET reporter) to red plus green (sum of intact reporter plus reduced reporter) fluorescence intensities were plotted against incubation time for folate-FRET reporter (●) and its thioether analog (○). The mean fluorescence intensity was measured for 10,000 cells by flow cytometry by using 488 nm excitation.

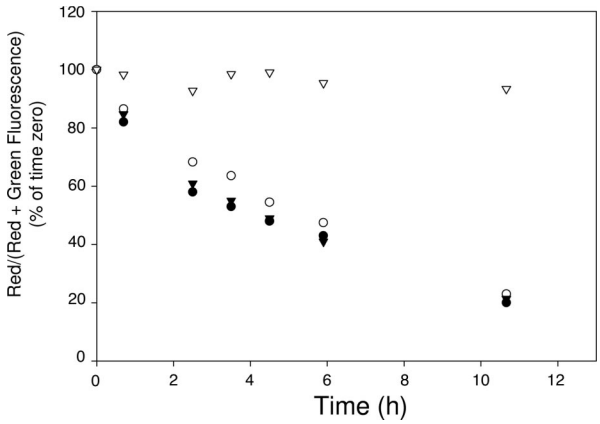

Fig. 3. Effect of SH blockers on disulfide cleavage of the folate-FRET conjugate in KB cells. Ratio of red to red plus green fluorescence in untreated (●), 5,5′-dithiobis-(2-nitrobenzoic acid) (○), or bacitracin-treated (triangles) cells was determined as described in Fig. 2 and plotted against incubation time. *N*-ethylmaleimide-treated (△) cells were analyzed for green and red fluorescence by quantitating the fluorescence intensities in the appropriate micrographs.

for disulfide reduction of 6 ± 1 h (n = 3 experiments). To ensure that the disappearance of FRET was not caused by mechanisms other than disulfide reduction (such as proteolysis-mediated destruction) of the folate-FRET reporter, an analogous conjugate was synthesized in which the disulfide bond (S-S) was replaced by a reduction-resistant thioether bond (S-C). When incubated similarly with KB cells, the thioether conjugate produced a nearly constant ratio of red to red plus green fluorescence over the observation period of 12 h. These data imply that disulfide bond reduction occurs within the folate trafficking pathway in a time-dependent fashion.

Evaluation of Potential Sites of Disulfide Reduction. As noted above, visual analysis of the gradual accumulation of green (reduced) folate-BODIPY fluorescence on the cell surface was incapable of distinguishing whether reduction had occurred initially at the cell surface or within an endosomal compartment before recycling back to the cell surface. Therefore, to assess where folate-FRET reduction begins, three SH blockers were compared for their effects on reduction of the folate conjugate. Pretreatment of the cells with *N*-ethylmaleimide (NEM), an irreversible and membrane-permeable SH reagent, was found to completely abolish conjugate reduction (Fig. 3), suggesting that free SHs are essential for cleavage of the disulfide bond. PDI, an exofacial thiol-dependent enzyme that has been previously shown to mediate disulfide cleavage (11), however, does not appear to be involved, because treatment with a PDI inhibitor (bacitracin) exerted no effect on the rate or extent of folate-FRET reduction (Fig. 3). More importantly, pretreatment with 5,5′-dithiobis-(2-nitrobenzoic acid), a membrane impermeable SH blocker, was unable to impede disulfide bond reduction (Fig. 3), suggesting that reduction of folate-FRET uses free thiols that are largely inaccessible at the cell surface.

Although the data in Fig. 1 *B–E* reveal that folate-FRET reduction can be seen by the time the conjugate has trafficked to the perinuclear region of the cell, the images do not allow evaluation of whether significant disulfide reduction proceeds before accumulation in this location. Therefore, to obtain a preliminary indication of whether expression of reducing activity requires translocation to the REC-like region of the cell, we inhibited collection of endosomes in the perinuclear region by treatment with colchicine and examined whether conversion of red to green fluorescence still occurred. As shown in Fig. 4 *A–C*, by 12 h after administration of the FRET reporter, essentially all folate conjugates had been reduced, i.e., similar to the results seen in control cells (Fig. 1 *B–E*), even though few of the endosomes had accumulated in the perinuclear region. To further confirm that this disulfide reduction proceeded in peripheral endocytic compartments without the assistance of recycling endosomes that might have relocated to the cell periphery upon microtubule disruption, we first loaded the recycling compartments with folate-rhodamine (red) and then treated

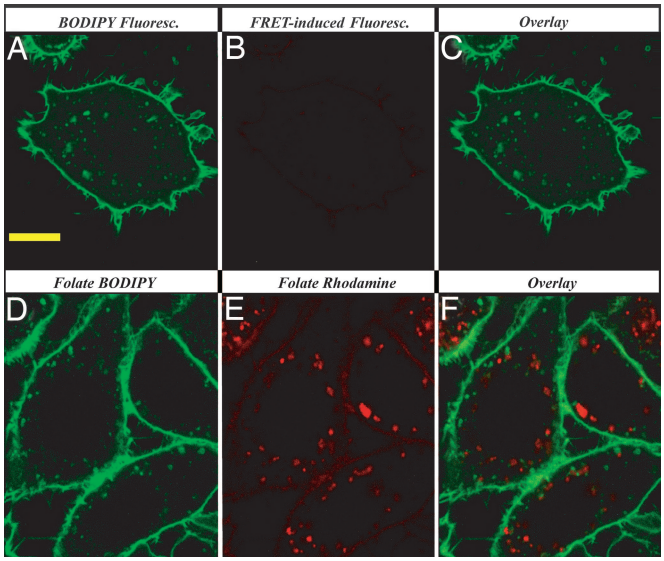

Fig. 4. Effect of colchicine on disulfide reduction of the folate-FRET reporter and FR recycling. (*A–C*) Disruption of microtubule network did not impede disulfide reduction of the folate-FRET reporter. KB cells were incubated with colchicine (10 μM) for 2 h at 37°C followed by a 0.5-h pulse with folate-FRET reporter (100 nM). After further incubation for 12 h in fresh medium, cells were imaged for BODIPY fluorescence (*A*) and FRET-induced fluorescence (*B*) (488/520 nm and 488/595 nm, respectively). (*C*) Overlay of *A* and *B*. (*D–F*) FR-containing endosomes do not merge with recycling compartments dispersed from the perinuclear region. Cells were treated for 2 h with folate-rhodamine to label the recycling center with the red dye, followed by rinsing with acidic buffer (pH 3.5) to remove surface-bound folate-rhodamine. Cells then were incubated with colchicine (10 μM) for 2 h to disrupt microtubules, followed by a 2-h treatment with folate-BODIPY to label newly internalized FR. Finally, cells were imaged for BODIPY (*D*) and rhodamine (*E*) fluorescence (488/520 nm and 543/595 nm, respectively). (*F*) Overlay of *D* and *E*. (Scale bar: 10 μm.)

the cells with colchicine to allow dispersion of the red FR-containing endosomes to the cell periphery. When folate-BODIPY (green) was subsequently added to these same cells, it was found to accumulate in endosomes that were void of red folate-rhodamine (Fig. 4 *D–F*), demonstrating that in the absence of a microtubule network, FR-containing endosomes do not merge with recycling compartments. Taken together, these data argue that trafficking of the endosomes to the recycling center is not required for disulfide reduction.

To determine whether disulfide reduction might depend on maturation of the folate-FRET-containing endosomes to lysosomes, we examined colocalization of the folate-FRET reporter with LysoSensor Yellow/Blue DND 160, a fluorescent lysosome marker ($pK_a = 4.2$). Importantly, at no time during endosomal trafficking was measurable overlap observed between folate conjugate fluorescence and lysosome staining (see Fig. 8*A*, which is published as supporting information on the PNAS web site), even though conversion of the red folate-FRET reporter to its reduced green counterpart proceeded normally. These data dismiss the lysosome as a significant site for reduction of the folate-FRET reporter.

Finally, cells were treated with brefeldin A to explore whether trafficking between the Golgi/trans-Golgi network (TGN) and folate-containing endosomes might contribute to disulfide bond reduction. Although brefeldin A induced the anticipated collapse of the Golgi network into a cortical assembly of endoplasmic reticulum vesicles, no interruption of disulfide bond reduction could be detected (Fig. 8*B*). Additional studies with BODIPY FL C_5-ceramide showed that the folate conjugate and this Golgi/TGN marker are localized to distinct compartments in the juxtanuclear region, suggesting that the folate receptor does not reach the Golgi/TGN during intracellular trafficking (Fig. 8*C*). Taken together, the above data argue that reduction can begin upon internalization of the folate-FRET reporter into endosomes and can proceed unabated in the absence of measurable interaction with either lysosomes or the Golgi apparatus.

Sorting of Folate-BODIPY from Released Free Rhodamine After Disulfide Bond Reduction. It is well established that acidic conditions (pH < 4.5) are required for dissociation of folic acid or its conjugates from the folate receptor (19). Therefore, after intraendosomal disulfide reduction, the folate-BODIPY fragment might be predicted to remain attached to the folate receptor, whereas the free rhodamine should be released into the endosomal lumen. To test this hypothesis, we compared the distributions of folate-BODIPY and rhodamine 12 h after initiation of incubation with the folate-FRET reporter. Importantly, FRET imaging was performed on all samples before the above analyses to confirm that disulfide reduction had reached completion by this time point (data not shown). For the purpose of these analyses, the 543-nm line of a He-Ne laser was used to directly excite free rhodamine, whereas the 488-nm line of the argon laser was used to illuminate folate-BODIPY. As shown in the higher magnification images of Fig. 5 *A* and *B*, the green fluorescence of the reduced folate-BODIPY often was seen to localize to "ring-like" structures in the cell interior, whereas the red fluorescence of the free rhodamine was commonly observed in the lumens of the same organelles. This distribution pattern of fluorophores was confirmed directly by quantitation of both fluorescence intensities along a single transept that traversed the examined vesicle. As seen in Fig. 5*C*, the intensity of green fluorescence exhibited two distinct peaks along the transept, whereas the intensity of red fluorescence reached a single maximum halfway between the two green fluorescence maxima. Importantly, some endosomes in the REC region could be seen to contain only released rhodamine with no associated folate-BODIPY (Fig. 5 *A* and *B*, see arrows), suggesting that the released rhodamine can be sorted into distinct vesicles from the folate-BODIPY fragment (see also Fig. 9, which is published as supporting information on the PNAS web site). More interesting, however, this sorting still was observed when trafficking of the endosomes to the perinuclear region was blocked by disruption of the cell's microtubules. Thus, as shown in Fig. 5 *D–F*, pretreatment of the cells with colchicine had little effect on separation of the two reduction products into distinct compartments, even though it clearly prevented trafficking of the conjugate-containing endosomes to the cell's center.

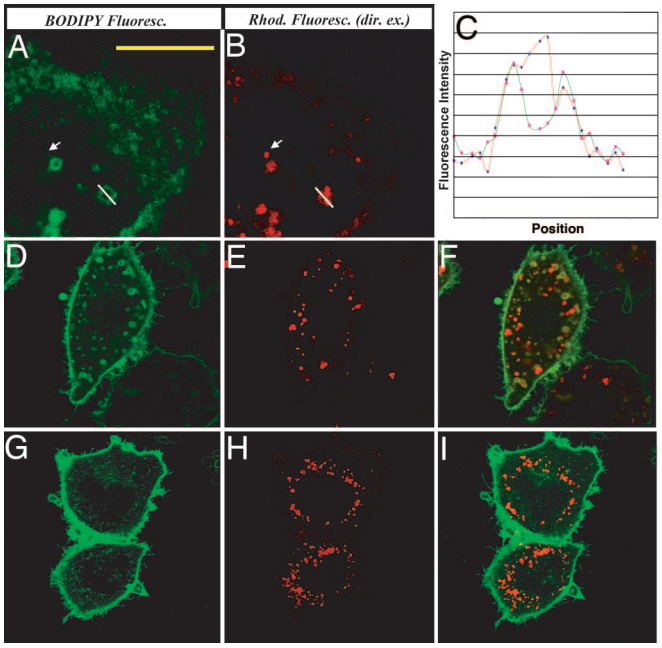

Fig. 5. Sorting of the reduction products of the folate-FRET reporter after disulfide reduction. (*A–C*) Release and sorting of rhodamine from folate-FRET reporter in endosomes. KB cells were treated first with folate-FRET for 0.5 h and then incubated in fresh medium for 12 h. Cells were then imaged for the reduced folate-BODIPY fragment (*A*) and the released rhodamine (*B*) by direct excitation of both dyes (488/520 nm and 543/595 nm, respectively). (*C*) Intensities of both BODIPY (green) and rhodamine (red) fluorescence along a transept across the marked endosome (indicated by a white line in *A* and *B*). Arrows indicate the endosomes containing only released rhodamine. (*D–F*) Effect of colchicine on the sorting of folate-BODIPY from released rhodamine. Cells were first treated with colchicine (10 μM) for 2 h before a 0.5-h pulse with folate-FRET reporter. After further incubation for 12 h, cells were imaged for reduced folate-BODIPY (*D*) and released rhodamine (*E*) by direct excitation of both dyes as described above. (*F*) Overlay of *D* and *E*. (*G–I*) Long-term effect of colchicine on sorting of folate-BODIPY from released rhodamine. Cells were treated as in *D–F* except incubation in fresh medium was continued for 24 h after washing to remove unbound ligands. Cells were then imaged for folate-BODIPY (*G*) and released rhodamine (*H*) by direct excitation at 488 nm and 543 nm, respectively. (*I*) Overlay of *G* and *H*. (Scale bar: 10 μm.)

Further, when the sorting process was allowed to continue for 24 h (Fig. 5 *G–I*), the folate-BODIPY was seen to localize primarily to the plasma membrane, whereas the released rhodamine was retained in the peripheral vesicles where they were first observed. It thus would appear that although colchicine treatment can inhibit trafficking of the released rhodamine-containing vesicles to the perinuclear region of the cell, it does not block recycling of the FR-containing endosomes to the plasma membrane.

Finally, to explore the relevance of our results to a better characterized endocytic pathway, namely transferrin receptor(TfR)-mediated endocytosis, colocalization of our folate-FRET conjugate with transferrin (Tf) was examined. As shown in Fig. 6, reduction products of the folate-FRET reporter (i.e., folate-BODIPY and free rhodamine) both were found to colocalize with Tf-containing endosomes. However, as shown by others (14), our micrographs did not reveal any case where the two cell-surface

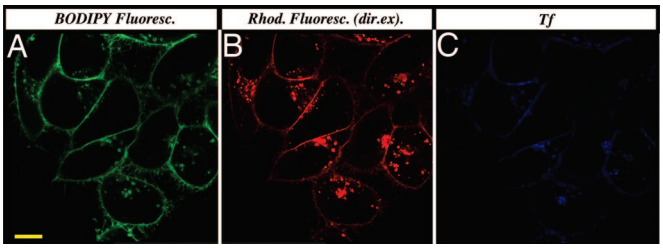

Fig. 6. Comparison of the trafficking pathways of folate-FRET reporter and transferrin (Tf) after endocytosis. Cells were treated with folate-FRET (100 nM) and Tf-Alexa 633 (5 μg/ml) for 0.5 h. After washing and further incubation for 6 h in fresh medium, cells were imaged for the folate-BODIPY fragment (*A*), rhodamine (*B*), and transferrin Alexa 633 (*C*) (488/520 nm, 543/595 nm, and 633/670 nm, respectively). (Scale bar: 10 μm.)

ligands internalized at the same site on the plasma membrane (data not shown). Regardless of where convergence might have occurred, the observed colocalization suggests that some of the conclusions derived from this study may apply to other endocytic pathways in mammalian cells.

Discussion

In this study, we have described a FRET-based imaging method that allows the monitoring of disulfide cleavage in live cells without invasive manipulations. Because neither cell disruption nor organelle isolation was required, we believe that the FRET methodology permits a more accurate assessment of disulfide bond reduction during normal vesicle trafficking in a living cell. Using this tool, we have demonstrated that the disulfide reduction machinery: (*i*) does not significantly depend on exofacially exposed SHs or surface-associated protein disulfide isomerase activity; (*ii*) is active primarily after internalization of the receptor–ligand complex into an endosome, remains active along the entire FR endocytic pathway, and is not associated with any specific trafficking organelle; and (*iii*) does not rely on the migration of endocytic vesicles along microtubules, nor involve fusion with lysosomes or interaction with the Golgi network. Finally, we also have provided evidence that a sorting process occurs during FR-mediated endocytosis that can divert material from the receptor-recycling pathway even when microtubules are disrupted.

In biological systems, disulfide cleavage mostly occurs as a consequence of a thiol-disulfide exchange that requires the presence of a thiolate anion (S^-). However, deprotonation of thiols is thermodynamically disfavored ($pK_a = 8.3$) in an acidic environment such as the endosome. As a result, a mechanism that exclusively depends on disulfide exchange with small thiol-containing compounds (e.g., glutathione) cannot account for the observed reduction of the folate-FRET reporter. It is also unlikely that a thiol-disulfide oxidoreductases (e.g., protein disulfide isomerase, thioredoxin, etc.) is responsible for folate-FRET reduction, because these enzymes typically exhibit optimal activities around neutral pH. Nonetheless, existence of an endosomal redox function is strongly implied by studies of transferrin-mediated iron uptake pathways in mammalian cells. Upon internalization of the Fe^{3+}–Tf–TfR complex into an endosome, Tf undergoes a conformational change that leads to dissociation of the iron from the complex. Although Tf-TfR recycles back to the cell surface for another round of iron uptake, the internalized iron is transported across the endosomal membrane by a divalent metal transporter, DMT1, which (as its name suggests) only accepts Fe^{2+} (20). Therefore, a redox function must exist in Tf-containing endosome to account for the conversion of Fe^{3+} to Fe^{2+}. Still, despite this evidence for reductase activity in the Tf cycle, the molecular identity of such machinery remains elusive. Recent work has suggested that six-transmembrane epithelial antigen of the prostate 3 (*Steap3*) may be responsible for iron reduction in the Tf endosome of erythroid cells (21). The fact that FR is largely colocalized with TfR rapidly after endocytic uptake (22) argues that endosomal ferrireducase also could participate in the observed reduction of the folate-FRET (probably with the assistance of another reduced cofactor as an electron donor).

Although in the presence of trafficking inhibitors (e.g., colchicine and brefeldin A) sorting of the released free rhodamine from folate-BODIPY upon disulfide reduction was observed in the cell periphery, under normal conditions, this sorting did not occur until the reduced components reach the perinuclear region. However, in neither case could trafficking of either fragment of the folate-FRET reporter be traced to a lysosomal compartment (Fig. 8). This observation was somewhat surprising, because current trafficking models suggest that nonrecycling ligands are diverted from the recycling pathway (e.g., Tf cycle) at the transient "sorting endosome" shortly after endocytosis and later delivered into peripherally located late endosomes and/or lysosomes. However, sorting near or within the REC already has been suggested by others. For example, Mayor *et al.* (15, 16) have demonstrated that the mechanism by which TfR returns from the REC to the cell surface more rapidly than FR is that the two receptors are sorted into distinct compartments at this site, and FR is retained in the REC by a glycosylphosphatidylinositol-dependent mechanism. Taken together, these observations argue that REC constitutes a branch point in the receptor-mediated recycling pathway, where a cell can prevent materials (e.g., released ligands, solute molecules, etc.) from being returned to the excellular space by sorting them into a distinct compartment that is retained inside the cell.

As noted above, we also have demonstrated that the folate-BODIPY fragment is trafficked back to the plasma membrane (presumably bound to FR) after disulfide reduction in colchicine-treated KB cells, suggesting that sorting and recycling of FR can proceed unabated in the absence of a functional microtubule network. This finding raises the question of whether efficient sorting/recycling, in fact, requires involvement of the recycling center, which is normally reached only by vesicle trafficking along microtubules. Data presented in Fig. 4 indeed demonstrate that sorting/recycling in colchicine-treated cells does not require the conventional recycling compartment. Apparently, sufficient recycling machinery is available in early endosomes to allow some degree of membrane recycling. We also speculate that some type of tether may exist between these peripherally stalled vesicles and the plasma membrane that enables the return of the FR-containing endosome back to the cell surface (23, 24).

The information gleaned from this study also may be relevant to researchers interested in ligand-targeted drug delivery. Because of elevated expression of FR on various types of tumor cells and activated macrophages, folic acid has been exploited extensively as a drug delivery vehicle for cancer and inflammatory diseases (25–29). Because higher potencies are achieved generally when the drug is released from its attached targeting ligand (i.e., folic acid) in an unaltered form (30–33), the data presented here suggest that disulfide bridges between folate and its therapeutic payload might constitute suitable linkers for site-specific drug release. This argument is supported by the much more potent antitumor activity of a disulfide-linked folate-mitomycin C conjugate relative to an analogus amide-linked conjugate (34, 35). Similarly, a disulfide-bridged folate-*Pseudomonas* exotoxin conjugate exhibited cytotoxicity that was four orders of magnitude more than the same conjugate connected by a thioether linkage (36). The benefit of redox-mediated release also has been shown by a variety of disulfide linked antibody-drug conjugates [C242-SPP-DM1 (37), anti-PSCA-DM1 (38), trastuzumab-SPP-DM1 (39), and gemtuzumab ozogamicin (40)].

Finally, during preparation of this manuscript, a report was published (41) showing that a disulfide bond in the Trastuzumab-(S-S)-rhodamine red conjugate was not significantly reduced after

endocytosis by breast carcinoma SKBr3 cells, suggesting a lack of redox function in the HER2-trafficking pathway. However, whether this inefficient processing of the disulfide could have derived from (*i*) different redox properties peculiar to the HER2 endosomal trafficking pathway or (*ii*) a lack of interaction between their macromolecular antibody conjugate and the endosomal redox enzymes responsible for disulfide reduction cannot be resolved from their data.

Materials and Methods

Materials, Cell Lines, and Synthesis of the Folate-FRET Reporter. See *Supporting Text* and Fig. 10, which are published as supporting information on the PNAS web site.

Characterization of Disulfide Bond Reduction of Folate-FRET Reporter in a Cell-Free System. See Fig. 7 legend for details.

Laser Imaging and Flow Cytometry. FRET imaging was performed by using an Olympus (Melville, NY) IX-70 inverted confocal microscope system. KB cells were incubated with folate-FRET reporter (100 nM) for 0.5 h on ice, followed by washes with fresh culture medium to remove any unbound folate-FRET molecules. Cells then were incubated at 37°C for the desired lengths of time (0.5–12 h) and examined with an Olympus 60X/1.2 NA water objective together with the appropriate filter sets (BODIPY, excitation 488 nm, emission 520/40; rhodamine, excitation 543 nm, emission 600/70; FRET, excitation 488 nm, emission 520/40, emission 600/70; Tf Alexa 633, excitation 633 nm, emission 670/40). Both BODIPY and FRET images of cells incubated with folate-BODIPY alone, and rhodamine and FRET images of cells exposed to folate-rhodamine were also obtained to determine bleed-through and background corrections. Images were processed by using FLUOVIEW (Olympus, Melville, NY).

Flow cytometric measurements were conducted to determine the rates of reduction of the folate-FRET by KB cells with a Becton Dickinson FACS caliber flow cytometer. Cells were incubated with either folate-FRET reporter (100 nM) or its nonreducible thioether analog (100 nM) for 0.5 h before washing. After further incubation for 0 to 12 h, cells were resuspended in PBS and subjected to flow cytometry. Using the 488-nm line of an argon ion laser to excite the donor (BODIPY), emission was measured at both 530 nm (to assay donor fluorescence from BODIPY) and 595 nm (to assay FRET-induced acceptor fluorescence from rhodamine). Correction factors for spectral overlap between the different fluorescence channels were obtained from single-labeled cells. The ratio of red (intact FRET reporter) to red plus green (sum of intact reporter plus reduced reporter) was calculated from the mean fluorescence intensity of 10,000 cells. CELLQUEST (Becton Dickinson, San Jose, CA) was used for acquiring and analyzing the data. SIGMAPLOT was used to plot the data and calculate reduction half time.

Inhibition of Cellular Redox Reactions. 5,5′-Dithiobis-(2-nitrobenzoic acid) (100 μM), bacitracin (1 mM), and *N*-ethylmaleimide (10 μM) were used to inactivate cell surface sulfhydryl groups, plasma membrane-associated PDI, and total cellular sulfhydryl groups, respectively, by treating KB cells with these inhibitors for 1 h at 37°C. Folate-FRET reporter (100 nM) then was added, and after 0.5 h of incubation, cells were washed and analyzed as described above. When desired, cells were incubated with inhibitor-containing medium for additional lengths of time, as indicated, before analysis by FRET imaging or flow cytometry.

Disruption of the Golgi Network and Localization of Lysosomes. See Fig. 10 legend for details.

Inhibition of Intracellular Trafficking of FR and Labeling of TfR Endocytic Pathway. When desired, cells were incubated for 2 h at 37°C with 10 μM colchicine to disrupt intracellular trafficking along microtubules. Cells then were incubated with folate-FRET reporter for 30 min before washing with fresh medium. Colchicine then was added back to the medium, and cells were incubated for the indicated hours before imaging.

Localization of TfR and FR in the same cells was performed by incubating KB cells simultaneously with folate-FRET reporter (100 nM) and transferrin-Alexa 633 (5 μg/ml) for the desired times before imaging.

We thank Drs. Santhapuram Hari Krishna and Chunhong Li and Mr. Stephen Howard for their advice on the synthesis of the folate-FRET reporter and Dr. Christopher Leamon for insightful discussions. Part of the microscopy was conducted at the Purdue University Cytometry Laboratories.

1. Meister A, Anderson ME (1983) *Annu Rev Biochem* 52:711–760.
2. Darby NJ, Freedman RB, Creighton TE (1994) *Biochemistry* 33:7937–7947.
3. Holmgren A, Bjornstedt M (1995) *Methods Enzymol* 252:199–208.
4. Holmgren A (1989) *J Biol Chem* 264:13963–13966.
5. Hwang C, Sinskey AJ, Lodish HF (1992) *Science* 257:1496–1502.
6. Blewitt MG, Chung LA, London E (1985) *Biochemistry* 24:5458–5464.
7. Falnes PO, Olsnes S (1995) *J Biol Chem* 270:20787–20793.
8. Ryser HJ, Mandel R, Ghani F (1991) *J Biol Chem* 266:18439–18442.
9. Falnes PO, Sandvig K (2000) *Curr Opin Cell Biol* 12:407–413.
10. Feener EP, Shen WC, Ryser HJ (1990) *J Biol Chem* 265:18780–18785.
11. Mandel R, Ryser HJ, Ghani F, Wu M, Peak D (1993) *Proc Natl Acad Sci USA* 90:4112–4116.
12. Antony AC (1996) *Annu Rev Nutr* 16:501–521.
13. Sabharanjak S, Mayor S (2004) *Adv Drug Delivery Rev* 56:1099–1109.
14. Sabharanjak S, Sharma P, Parton RG, Mayor S (2002) *Dev Cell* 2:411–423.
15. Mayor S, Sabharanjak S, Maxfield FR (1998) *EMBO J* 17:4626–4638.
16. Chatterjee S, Smith ER, Hanada K, Stevens VL, Mayor S (2001) *EMBO J* 20:1583–1592.
17. Kennedy MD, Jallad KN, Lu J, Low PS, Ben-Amotz D (2003) *Pharm Res* 20:714–719.
18. Kennedy MD, Jallad KN, Thompson DH, Ben-Amotz D, Low PS (2003) *J Biomed Opt* 8:636–641.
19. Kamen BA, Smith AK (2004) *Adv Drug Delivery Rev* 56:1085–1097.
20. Gunshin H, Mackenzie B, Berger UV, Gunshin Y, Romero MF, Boron WF, Nussberger S, Gollan JL, Hediger MA (1997) *Nature* 388:482–488.
21. Ohgami RS, Campagna DR, Greer EL, Antiochos B, McDonald A, Chen J, Sharp JJ, Fujiwara Y, Barker JE, Fleming MD (2005) *Nat Genet* 37:1264–1269.
22. Turek JJ, Leamon CP, Low PS (1993) *J Cell Sci* 106:423–430.
23. Rothberg KG, Ying YS, Kolhouse JF, Kamen BA, Anderson RG (1990) *J Cell Biol* 110:637–649.
24. Lewis CM, Smith AK, Kamen BA (1998) *Cancer Res* 58:2952–2956.
25. Paulos CM, Turk MJ, Breur GJ, Low PS (2004) *Adv Drug Delivery Rev* 56:1205–1217.
26. Zhao XB, Lee RJ (2004) *Adv Drug Delivery Rev* 56:1193–1204.
27. Lu Y, Sega E, Leamon CP, Low PS (2004) *Adv Drug Delivery Rev* 56:1161–1176.
28. Ke CY, Mathias CJ, Green MA (2004) *Adv Drug Delivery Rev* 56:1143–1160.
29. Low PS, Antony AC (2004) *Adv Drug Delivery Rev* 56:1055–1058.
30. Garnett MC (2001) *Adv Drug Delivery Rev* 53:171–216.
31. Dubowchik GM, Walker MA (1999) *Pharmacol Ther* 83:67–123.
32. D'Souza AJ, Topp EM (2004) *J Pharm Sci* 93:1962–1979.
33. Dyba M, Tarasova NI, Michejda CJ (2004) *Curr Pharm Des* 10:2311–2334.
34. Leamon CP, Reddy JA, Vlahov IR, Vetzel M, Parker N, Nicoson JS, Xu LC, Westrick E (2005) *Bioconjug Chem* 16:803–811.
35. Reddy JA, Westrick E, Vlahov I, Howard SJ, Santhapuram HK, Leamon CP (2006) *Cancer Chemother Pharmacol* 58:229–236.
36. Leamon CP, Pastan I, Low PS (1993) *J Biol Chem* 268:24847–24854.
37. Liu C, Tadayoni BM, Bourret LA, Mattocks KM, Derr SM, Widdison WC, Kedersha NL, Ariniello PD, Goldmacher VS, Lambert JM, *et al.* (1996) *Proc Natl Acad Sci USA* 93:8618–8623.
38. Ross S, Spencer SD, Holcomb I, Tan C, Hongo J, Devaux B, Rangell L, Keller GA, Schow P, Steeves RM, *et al.* (2002) *Cancer Res* 62:2546–2553.
39. Ranson M, Sliwkowski MX (2002) *Oncology* 63(Suppl 1):17–24.
40. Giles F, Estey E, O'Brien S (2003) *Cancer* 98:2095–2104.
41. Austin CD, Wen X, Gazzard L, Nelson C, Scheller RH, Scales SJ (2005) *Proc Natl Acad Sci USA* 102:17987–17992.